Int J Clin Exp Pathol 2014;7(4):1337-1347
www.ijcep.com /ISSN:1936-2625/IJCEP1401079

Original Article

Increasing the cytotoxicity of doxorubicin in breast cancer MCF-7 cells with multidrug resistance using a mesoporous silica nanoparticle drug delivery system

Xin Wang[1], Zhaogang Teng[1], Haiyan Wang[2], Chunyan Wang[1], Ying Liu[1], Yuxia Tang[1], Jiang Wu[1], Jin Sun[1], Hai Wang[2], Jiandong Wang[2], Guangming Lu[1]

Departments of [1]Radiology, [2]Pathology, Jinling Hospital, Nanjing University School of Medicine, Nanjing, 210002, China

Received January 21, 2014; Accepted February 23, 2014; Epub March 15, 2014; Published April 1, 2014

Abstract: Resistance to cytotoxic chemotherapy is the main cause of therapeutic failure and death in women with breast cancer. Overexpression of various members of the superfamily of adenosine triphosphate binding cassette (ABC)-transporters has been shown to be associated with multidrug resistance (MDR) phenotype in breast cancer cells. MDR1 protein promotes the intracellular efflux of drugs. A novel approach to address cancer drug resistance is to take advantage of the ability of nanocarriers to sidestep drug resistance mechanisms by endosomal delivery of chemotherapeutic agents. Doxorubicin (DOX) is an anthracycline antibiotic commonly used in breast cancer chemotherapy and a substrate for ABC-mediated drug efflux. In the present study, we developed breast cancer MCF-7 cells with overexpression of MDR1 and designed mesoporous silica nanoparticles (MSNs) which were used as a drug delivery system. We tested the efficacy of DOX in the breast cancer cell line MCF-7/MDR1 and in a MCF-7/MDR1 xenograft nude mouse model using the MSNs drug delivery system. Our data show that drug resistance in the human breast cancer cell line MCF-7/MDR1 can be overcome by treatment with DOX encapsulated within mesoporous silica nanoparticles.

Keywords: Breast cancer, MSNs, MDR, drug delivery system

Introduction

Breast cancer is currently one of the most prevalent neoplasia, and around one in 10 Western women will develop breast cancer at some time in their life [1]. It is the second most common cause of cancer death in women, and despite radical mastectomy approximately one third of affected women die. At present, chemotherapy including adjuvant and neoadjuvant chemotherapy is the major treatment for breast cancer. Although chemotherapy improves survival rates in the adjuvant setting, around 50% of all treated patients will relapse. The major reason for therapeutic failure is the development of resistance against the anticancer agents used. The development of a multidrug resistance (MDR1) phenotype in advanced breast cancer is primarily responsible for the failure of current treatment regimens [2, 3]. Such a MDR1 phenotype can be intrinsic (primary) or acquired (secondary). Two types of MDR1 have been distinguished: P-glycoprotein-dependent and non-P-glycoprotein-dependent MDR1. P-glycoprotein is a member of the ABC (adenosine triphosphate binding cassette)-transporters superfamily. ABC-transporters act as energy-dependent drug efflux pumps, thereby decreasing the accumulation of cytotoxic agents in the intracellular millieu [4-6]. The most extensively studied mechanism of drug resistance is the P-glycoprotein-dependent phenotype characterized by a typical cross resistance pattern against natural product-derived anticancer agents, such as anthracyclines (doxorubicin and epirubicin are among the most effective cytotoxic drugs used in the treatment of breast cancer), epipodophyllotoxins, vinca alkaloids, or taxanes, and reversibility by the calcium channel inhibitor verapamil and cyclosporin A derivatives.

Strategies for overcoming P-glycoprotein-dependent MDR1 have been tested. Pharmacologically active drug resistance-reversing

compounds are designed as MDR1 modulators or chemosensitizers. One obstacle in applying MDR1 modulators arises from their intrinsic toxicity at doses necessary for activity, such as heart failure, hypotension, hyperbilirubinemia, bone-marrow and neurological toxicity. In addition, tumor cells can develop resistance to these chemosensitizers. Another approach to reverse drug resistance of MDR1 is the use of P-glycoprotein inhibitors. Verapamil was found to inhibit the function of P-glycoprotein and reverse drug resistance [7-10]. This discovery led to clinical trials which attempted to reverse drug resistance using agents such as amiodarone, cyclosporine, valspodar and VX710. Although significant progress has been made in reversing drug resistance using these strategies, clinical trials have mostly failed. Thus, it is necessary to explore new approaches to reverse drug resistance in breast cancer.

Nanotechnology has been widely used in biology and medicine for anticancer therapy. The nanoparticle-based drug delivery systems offer numerous advantages including low toxicity, controlled release of drugs, and the ability to target cancer cells with cancer specific molecules [11-17]. Construction of a nanoparticle-based drug delivery system to bypass the efflux action of P-glycoprotein has been proven to be a promising approach to reverse drug resistance [18, 19]. Doxorubicin (DOX) is anthracycline antibiotic commonly used in breast cancer chemotherapy and a substrate for MDR1-mediated drug efflux. We designed mesoporous silica nanoparticles (MSNs) for cancer diagnosis and therapy. In the present study, we tested the efficacy of DOX in the breast cancer cell line MCF-7/MDR1 and in a MCF-7/MDR1 xenograft nude mouse model using the MSNs drug delivery system.

Materials and methods

Development and characterization of MCF-7/MDR1 cells

The drug-resistant MCF-7/MDR1 cell line was derived from MCF-7 cells purchased from the American Type Culture Collection (ATCC, Manassas, VA, USA) by selection with the chemotherapeutic DOX. According to a previous report [20], we developed DOX-resistant MCF-7 cells (MCF-7/MDR1) by exposing MCF-7 cells to increasing doses of DOX (1, 5, 10, 25, 50, 100, 500, 1000, 5000 ng/mL) for 24 h followed by 3-4 days of recovery before exposure to the next dose. MCF-7/MDR1 cells were then frozen and stored in liquid nitrogen. Fresh aliquots of MCF-7/MDR1 cells were used in all experiments to ensure that these cells did not revert to a drug sensitive phenotype. The DOX dose reducing viability by 50% (IC_{50}) was more than 20-fold greater in MCF-7/MDR1 cells than in their wild-type progenitors.

The mRNA of MDR1 was determined in MCF-7 control cells and MCF-7/MDR1 cells by quantitative real-time RT-PCR. The total RNA in MCF-7 and MCF7/MDR1 cells was extracted. The expression level of MDR1 mRNA in MCF7 and MCF7/MDR1 cells was determined by a quantitative real-time RT-PCR using the Applied Biosystems 7500 (850 Lincoln Centre Drive Foster City, CA 94404 USA) with specific primer sets to MDR1 gene as follows: MDR1 forward primer: 5-TGACATTTATTCAAAGTTAAAAGCA-3, MDR1 reverse primer: 5-TAGACACTTTATGCAAACATTTTCAA-3. The house keeping gene glyceraldehyde-3-phosphate dehydrogenase (GAPDH) was used as an internal control. GAPDH forward primer: 5'-GCAGGGGGGAGCCAAAAGGGT-3' and reverse primer: 5'-TGGGTGGCAGTGATGGCATGG-3'.

We determined the MDR1 protein in MCF-7 control cells and MCF-7/MDR1 cells to characterize drug resistance in the cell line using western blot assay, immunohistochemical staining and fluorescent immunohistochemical staining with a MDR1 specific antibody. For the western blot assay, cells were lysed using lysis buffer, and then equivalent amounts of protein were loaded and electrophoresed on 8% gradient SDS-PAGE gel and transferred to a nitrocellulose transfer membrane (PROTRAN Whatman, Germany). After blocking the membrane, it was probed with primary antibodies against MDR1 (Santa Cruz Biotechnology, Dallas, USA, diluted 1:200), and alpha-tubulin (Cell Signaling Technology, Boston, USA, diluted 1:1000) at 4°C overnight. Thereafter, the blots were washed, and then incubated with horseradish peroxidase conjugated secondary antibodies. Finally, immunoreactive bands were visualized using chemiluminescence (Thermo Scientific, Waltham, USA).

Preparation and physicochemical characteristics of MSNs

The rod-like MSNs were synthesized using procedures according to those previously pub-

Equation 1:

$$\text{Drug entrapment efficiency}(\%) = \frac{\text{initial weight of DOX - weight of DOX in supernatant solution}}{\text{initial weight of DOX}} \times 100\%$$

lished [21-23]. Typically, 0.53 mmol CTAB and 0.016 μmol PFOA were dissolved in deionized 96 g H_2O. After stirring for 1 h, 0.7 mL NaOH aqueous solution (2 M) was added. The temperature of the solution was increased to 80°C. Then 6.3 mmol TEOS was added to the above mixture dropwise within 3 min under steady stirring at about 600 rpm. The solution was stirred for another 2 h. The products were collected by centrifugation and washed with ethanol. The as-synthesized nanoparticles were dispersed in ethanolic HCl to remove the surfactant from the mesopores. The solvent-extracted particles were collected by centrifugation, washed with ethanol, and dried under vacuum. The structures of MSNs were characterized using transmission electron microscopy (JEOL JEM-2100, Japan) operated at 200 kV. X-ray diffraction (XRD) patterns were recorded on an X'Pert Pro powder diffractometer equipped with Cu Kα radiation. N_2 adsorption-desorption isotherms were obtained at 77 K by using a Micromeritics ASAP Tristar II 2020 system. The samples were degassed at 453 K. The Brunauer-Emmett-Teller (BET) method was utilized to measure the specific surface areas. The pore size distribution curves were obtained from the adsorption branches of the isotherms by using the Barrett–Joyner–Halanda (BJH) method. The pore volume was measured from the amount adsorbed at a maximum relative pressure (P/P_0).

Drug loading and release

The mixed solution of 2 mg/mL MSNs and 0.5 mg/mL DOX in phosphate buffered saline (PBS) underwent ultrasound to obtain a homogeneous solution. HCl and NaOH were used for pH adjustment. The mixed loading solution was adjusted to pH 5.4, pH 6.4, and pH 7.4, respectively. After these loading solutions had been stirred for 24 h, the different DOX-loaded MSNs were centrifuged, washed three times with PBS and were named DMSN-5.4, DMSN-6.4, and DMSN-7.4, respectively. The drug entrapment efficiency was calculated using the following **Equation 1** [24].

The release profile was determined as previously reported [25]. The DOX-loaded MSNs were re-dispersed and transferred into a dialysis bag (cutoff molecular weight, 8,000~14,000 Da). The bag was placed in 40 mL of PBS solution at pH 7.4 (i.e. physiological environment), pH 6.5 or pH 5.6 and gently shaken. The volume of the release medium was kept constant by adding fresh medium after each collection. The release of DOX was observed over 2, 4, 8, 16, 20, and 24 h periods, respectively. The concentration of DOX was measured using a UV/VIS spectrometer (Lambda 35, PerkinElmer) and compared with the standard curve.

Evaluation of cytotoxicity of DOX delivered by MSNs in MCF-7/MDR1 cells

The cellular internalization of DOX and DMSN-7 in MCF-7 and MCF-7/MDR1 cells was observed and assessed by photography after incubation with free DOX or equivalent DMSN-7 at 18.3 μg/mL. After 6 h incubation, the cells were washed thrice with PBS and fixed with 4% paraformaldehyde solution for 20 min, then washed thrice with PBS. For detection of DOX, λex = 520 nm and λem = 580 nm filter sets were used. The quantitative evaluation of free DOX and DMSN-7 cellular internalization was performed under a fluorescence microscope (Olympus I×71, Japan) at ×400 magnification and the fluorescent intensity of DOX was measured with Image Pro Express software (Media Cybernetics, USA).

The *in vitro* cytotoxicity of DMSNs was tested via terminal deoxynucleotidyl transferase-mediated dUTP nick end labeling (TUNEL) assay and cell viability by MTT assay. TUNEL assay was also used to detect apoptosis [7]. Cell apoptosis after drug treatment was determined by TUNEL assay using the in situ cell death detection kit-POD (Roche, Burgess Hill, UK) according to the manufacturer's instructions. Photographs of apoptosis of the two cell lines were recorded under a X fluorescence microscope at ×100 magnification.

A total of 5×10^3 cells in 100 μL medium were plated into each well of a 96-well plate. Cells were incubated at 37°C for 2 h. The supernatant was carefully removed, 100 μL medium and 10 μL of a 5 mg/mL MTT solution were

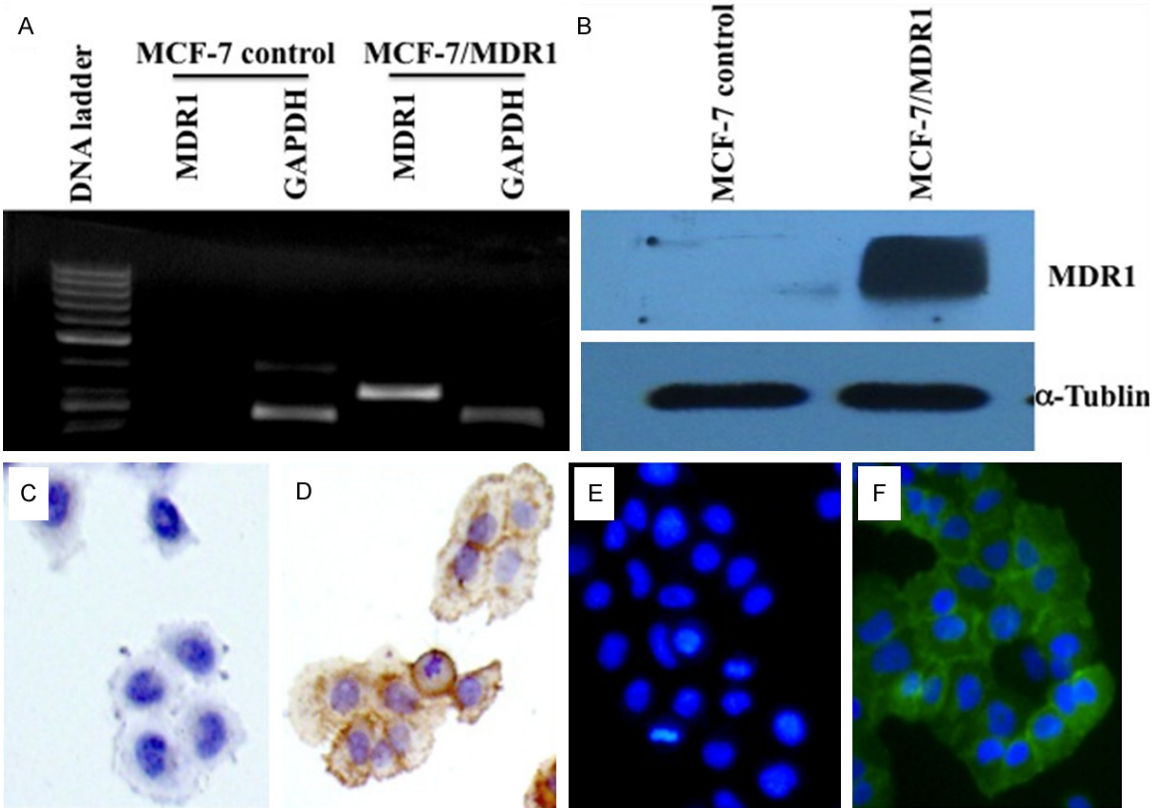

Figure 1. High expression of MDR1 in MCF-7/MDR1 breast cancer cells. (A) MDR1 mRNA was expressed in MCF-7/MDR1 cells, but not in MCF-7 control cells. The house keeping gene GAPDH was used as an internal control of gene expression. (B) MDR1 protein was detected in MCF-7/MDR1 cells, but not in MCF-7 control cells. The house keeping gene-tubulin was used as an internal control. (C and D) MDR1 protein was not positively stained in MCF-7 control cells (C), but was positively stained in the cellular membrane and cytoplasm of MCF-7/MDR1 cells by immunohistochemical staining (D). (E and F) MDR1 protein was positively stained in the cellular membrane and cytoplasm in MCF-7/MDR1 cells using fluorescent immunohistochemical staining.

added and incubated for a further 3 h. Viable cells internalize MTT into their mitochondria and metabolize it into blue formazan crystals. The supernatant in each well was aspirated and 100 μL dimethyl sulfoxide (DMSO) was added to solubilize cells and MTT crystals. After 4 h of shaking on an Eppendorf Thermomixer at 37°C and 400 rpm to dissolve all crystals, the blue color was determined using a multiwall scanning spectrophotometer at a wavelength of 490 nm.

Tumor animal model and in vivo treatment

Athymic BALB/c nu/nu female mice (6 weeks) were housed and received humane care in compliance with the Guide for the Care and Use of Laboratory Animals of Nanjing University School of Medicine. The MCF-7/MDR1 cell suspension (0.2 mL, 5×10^7 cells/mL) was injected into the breast of mice. When tumor volumes were greater than 200 mm^3, the mice were randomly divided into three groups. The mice were administered (A) physiological saline, (B) DOX, and (C) DMSN-7 intratumorally every 5 days. The DOX concentration in group B and D was 3 mg/kg body weight. Mice were imaged at day 5 post-injection using the IVIS imaging system (Caliper Life Sciences). Three weeks post administration, they were euthanized according to the animal protocol, and their tumors were immediately collected and weighed.

Statistical analysis

All values are shown as the mean ± standard error of the mean. Statistical analysis was performed using the One-way ANOVA and a significant difference test using SPSS statistical software (SPSS version 15.0, SPSS Inc, Chicago, IL,

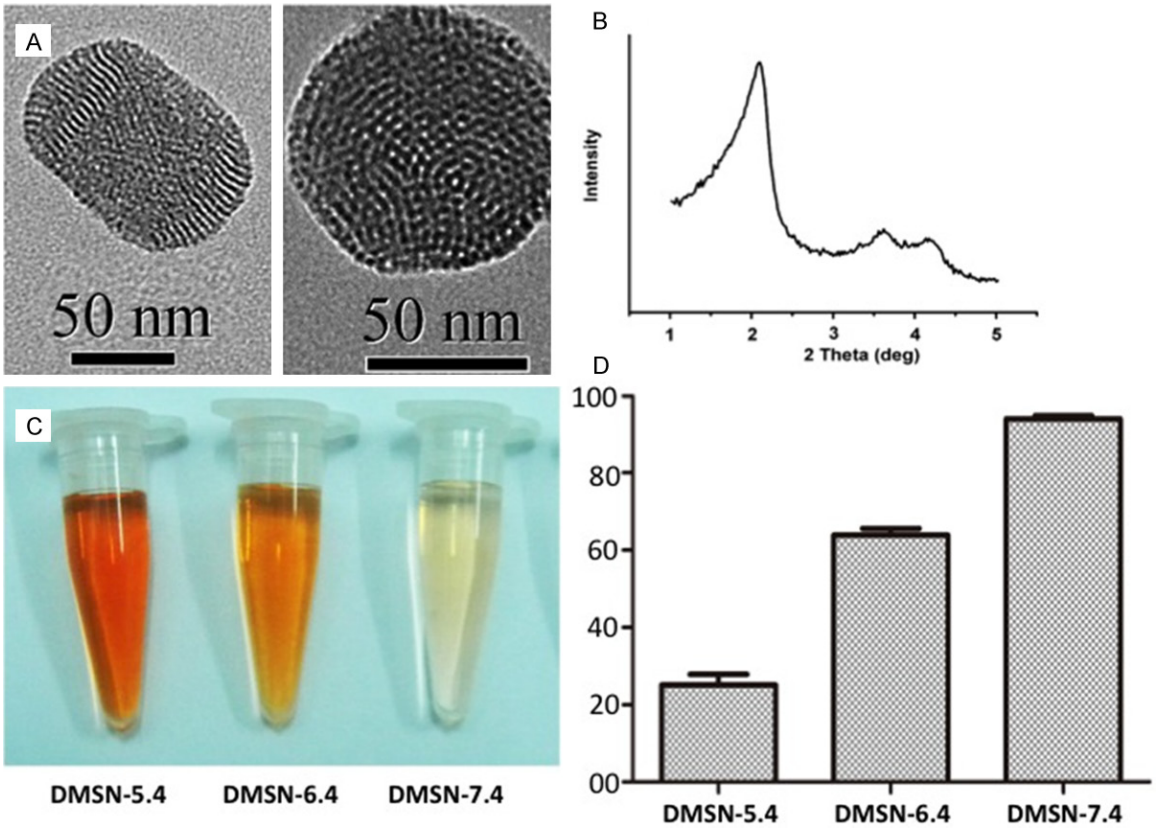

Figure 2. A. Transmission electron microscope image of MSNs exhibiting rod-shaped particles with a mean particle diameter of approximately 110 nm, uniform pore size of 2.7 nm and aspect ratio (AR) of 2.1-2.5. B. X-ray diffraction patterns of all the samples. The positions of the peaks represent the ordered hexagonal pore arrangements. C. The supernatant solutions of DMSN-5.4, DMSN-6.4, and DMSN-7.4 showed less color, respectively, indicating increased entrapment of DOX. D. The drug entrapment efficiency of DMSN-5.4, DMSN-6.4, and DMSN-7.4 increased by 25.2%, 63.8%, and 94.0%. There was a significant difference in entrapment of DOX with different solvent pH values (P<0.001).

USA). Statistical significance was defined as a P value≤0.05.

Results

High expression of MDR1 in MCF7/MDR1 cells

MDR1 mRNA was highly expressed in MCF7/MDR1 cells, but not in MCF7 control cells (**Figure 1A**). MDR1 protein was detected in MCF7/MDR1 cells, but not in MCF7 control cells by western blot (**Figure 1B**). In cell slides prepared from cultured cells, MDR1 protein was highly expressed in the cytoplasm and cellular membrane of MCF7/MDR1 cells, but was not expressed in MCF7 control cells (**Figure 1C-F**). Our data show that MDR1 was highly expressed in MCF7/MDR1 cells, but not in MCF-7 control cells.

Efficacy of DOX loading and release in the MSNs system depends on the solution pH

Transmission electron microscopy (TEM) images of the mesoporous silica nanospheres prepared using cetyltrimethylammonium bromide (CTAB) surfactant as a structure-directing agent revealed rod-shaped structures with a mean particle diameter of approximately 110 nm, uniform pore size of 2.7 nm and aspect ratio (AR) of 2.1-2.5. High-magnification TEM demonstrated the mesochannels of the spheres to be continuous throughout the shells with openings at the surface and fully oriented radially to the sphere surface, indicating readily accessible mesochannels that favor the adsorption and release of guest molecules (**Figure 2A**). X-ray diffraction patterns of all the samples are shown in **Figure 2B**. The positions of the peaks

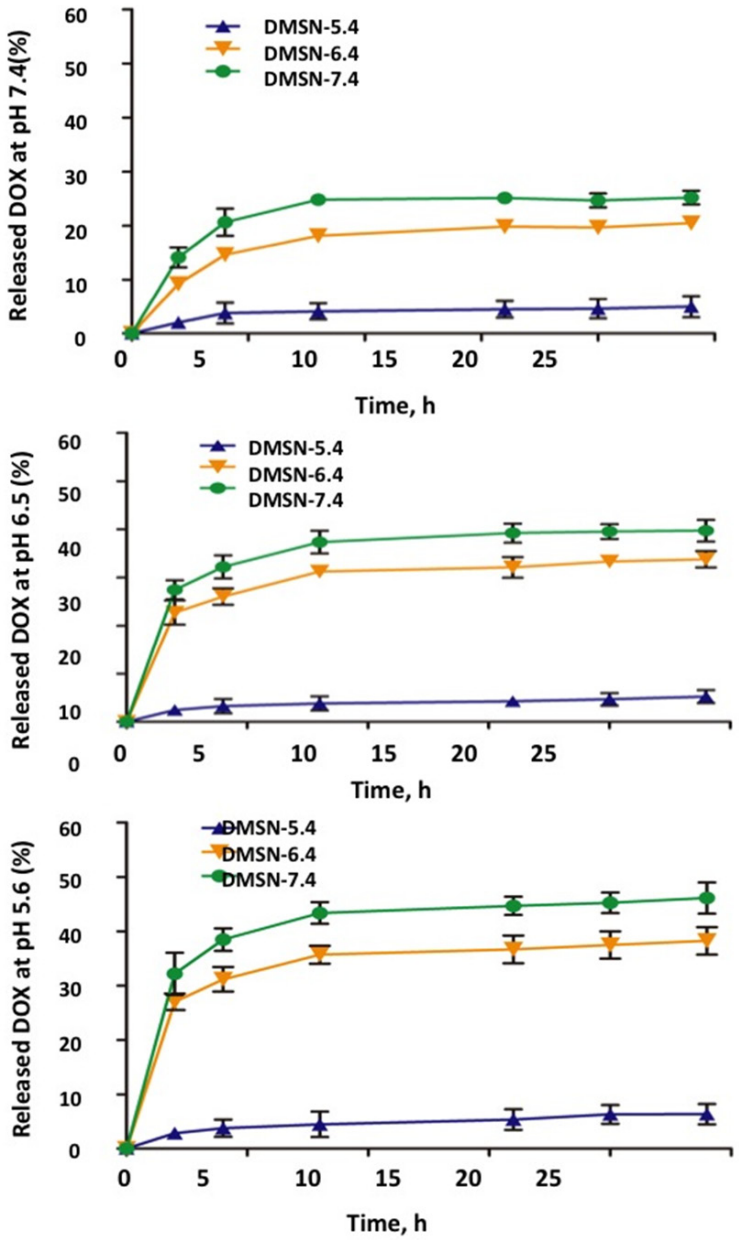

Figure 3. Drug release efficacy was investigated in a physiological pH condition (PBS, pH 7.4) and acidic environment (pH 6.5 and 5.6). At pH 7.4, DMSNs have a low release rate of DOX, while at pH 5.6 and 6.5 the DOX release rate is high. The cumulative drug release rate for DMSN-7.4 reached 46.1% and 39.7% at pH 5.6 and 6.5, respectively.

represent the ordered hexagonal pore arrangements.

We tested the PBS solvent at different pH values on the loading efficacy of DOX. The amount of drug loaded significantly depended on the pH value of the loading solution. The supernatant solutions of DMSN-5.4, DMSN-6.4, and DMSN-7.4 showed less color, respectively (**Figure 2C**). The drug entrapment efficiency of these samples increased by 25.2%, 63.8%, and 94.0%, respectively (**Figure 2D**). There was a significant difference in the entrapment of DOX with different solvent pH values ($P<0.001$). DMSN-7.4 had the highest drug entrapment efficiency.

The drug release efficacy was investigated in a physiological pH condition (PBS, pH 7.4) and acidic conditions (pH 6.5 and 5.6) (**Figure 3**). DOX release rate was higher in the acidic conditions than in the physiological pH condition. At pH 7.4, DMSNs had a low release rate of DOX, while at pH 5.6 and 6.5 the rate of DOX release was high. The accumulative drug release rate for DMSN-7.4 reached 46.1% and 39.7% at pH 5.6 and 6.5, respectively. These results suggest that the MSNs drug delivery system was favorable for DOX entrapment at physiological pH and release at acidic pH for reversal of MDR1.

The MSNs-DOX drug delivery system increases the cytotoxicity of DOX in MFC-7/MDR1 cells

Cellular internalization of DOX and DMSN-7.4 in MCF-7 and MCF-7/MDR1 cells was observed by fluorescence microscopy (**Figure 4A**). The quantitative evaluation of free DOX and DMSN-7.4 was performed by photography under a fluorescence microscope (Olympus I×71, Japan) at ×400 magnification and measured with Image Pro Express software (Media Cybernetics, USA). There was no difference in cellular internalization of DOX and DMSN-7.4 in MCF-7 cells (**Figure 4B**). Cellular internalization of DMSN-7.4 was greater than DOX in MCF-7/MDR1 cells ($P<0.001$) (**Figure 4C**).

TUNEL assays can efficiently detect cell apoptosis by labeling the terminal ends of nucleic acids of DNA fragments. As shown in **Figure 4D**, DMSN-7.4 was able to induce not only MCF-7

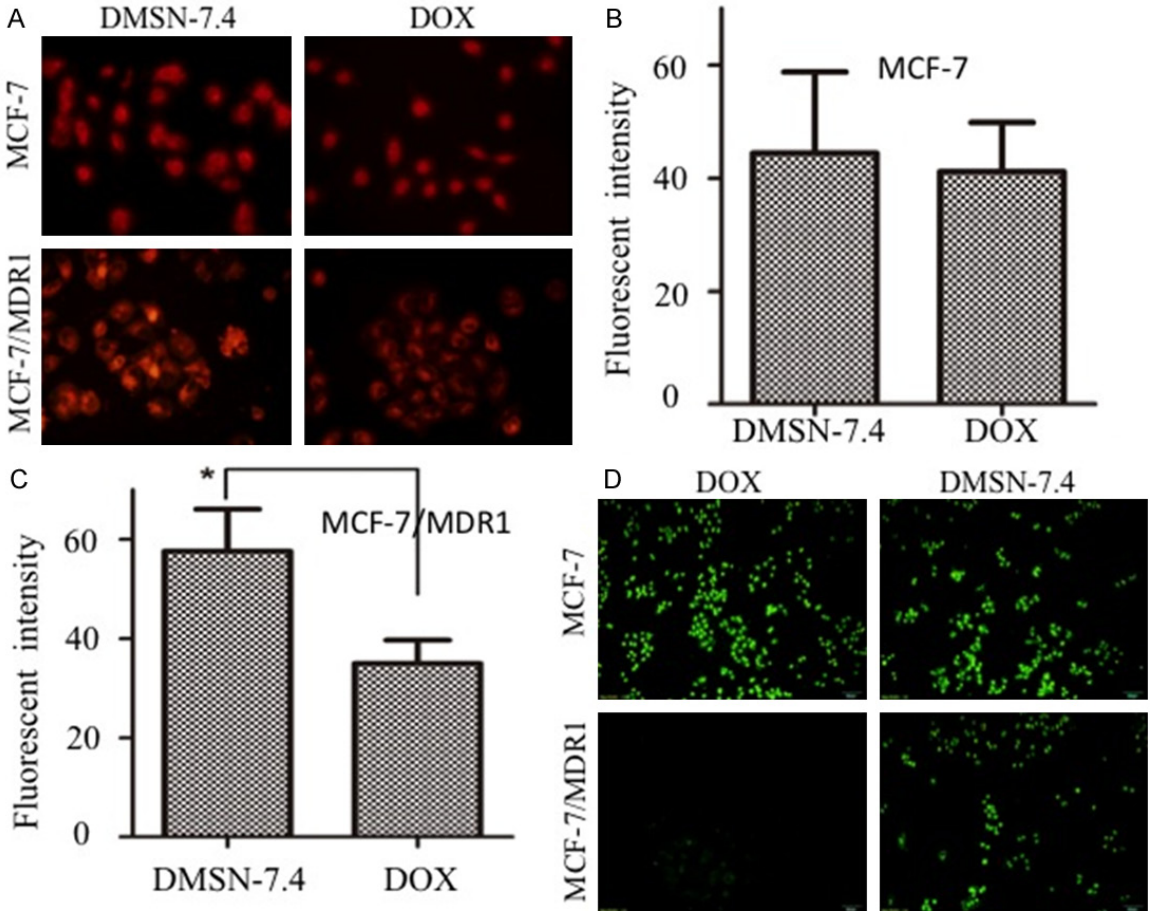

Figure 4. A. Cellular internalization of DOX and DMSN-7.4 in MCF-7 and MCF-7/MDR1 cells was observed by fluorescence microscopy. B and C. The quantitative evaluation of free DOX and DMSN-7.4 was performed by photography under a fluorescence microscope (Olympus I×71, Japan) at ×400 magnification and measured with Image Pro Express software (Media Cybernetics, USA). D. TUNEL assay showing apoptosis by free DOX and DMSN-7.4 in MCF-7 cells and MCF-7/MDR cells after 24 h incubation.

cell apoptosis, but also MCF-7/MDR cell apoptosis, whereas equivalent free DOX showed no obvious apoptosis fluorescence after 24 h incubation.

The cytotoxicity of MSNs was measured by MTT in both MCF-7 and MCF-7/MDR1 cells at different concentrations. MSNs exhibited limited toxicity with 71.4% cell viability of MCF-7 cells at 1600 μg/mL and negligible cytotoxicity at 800 μg/mL or lower (**Figure 5A**). MSNs exhibited no obvious cytotoxicity in MCF-7/MDR1 cells at the concentrations of 50 to 1600 μg/mL even after culturing for 48 h (**Figure 5B**). These data demonstrate the excellent biocompatibility of MSNs, which were safe at 800 μg/mL for both MCF-7 and MCF-7/MDR1 cells.

To determine whether DMSN-7.4 could reverse MDR1, the anticancer activities of free DOX and DMSN-7.4 were evaluated in MCF-7 control cells and MCF-7/MDR1 cells by MTT assays. Free DOX and DMSN-7.4 showed dose-dependent toxicity in MCF-7 and MCF-7/MDR1 cells (**Figure 5C** and **5D**). The half-maximum inhibitory concentration (IC_{50} value) of DMSN-7.4 was 7.38 μg/mL, whereas that of free DOX was 34.8 μg/mL in MCF-7/MDR1 cells. The cytotoxicity of DOX and DMSN-7.4 was similar in MCF-7 cells at all the concentrations tested (**Figure 5C**). The cytotoxicity of DMSN-7.4 was high in MCF-7/MDR1 cells at the higher concentrations of 5.8 and 18.3 mg/mL (P<0.001) (**Figure 5D**).

The MSNs-DOX drug delivery system increases therapeutic efficacy in vivo

To compare the therapeutic effect of free DOX and DMSN-7.4 nanoparticles, both formulations were administered at an equivalent dose

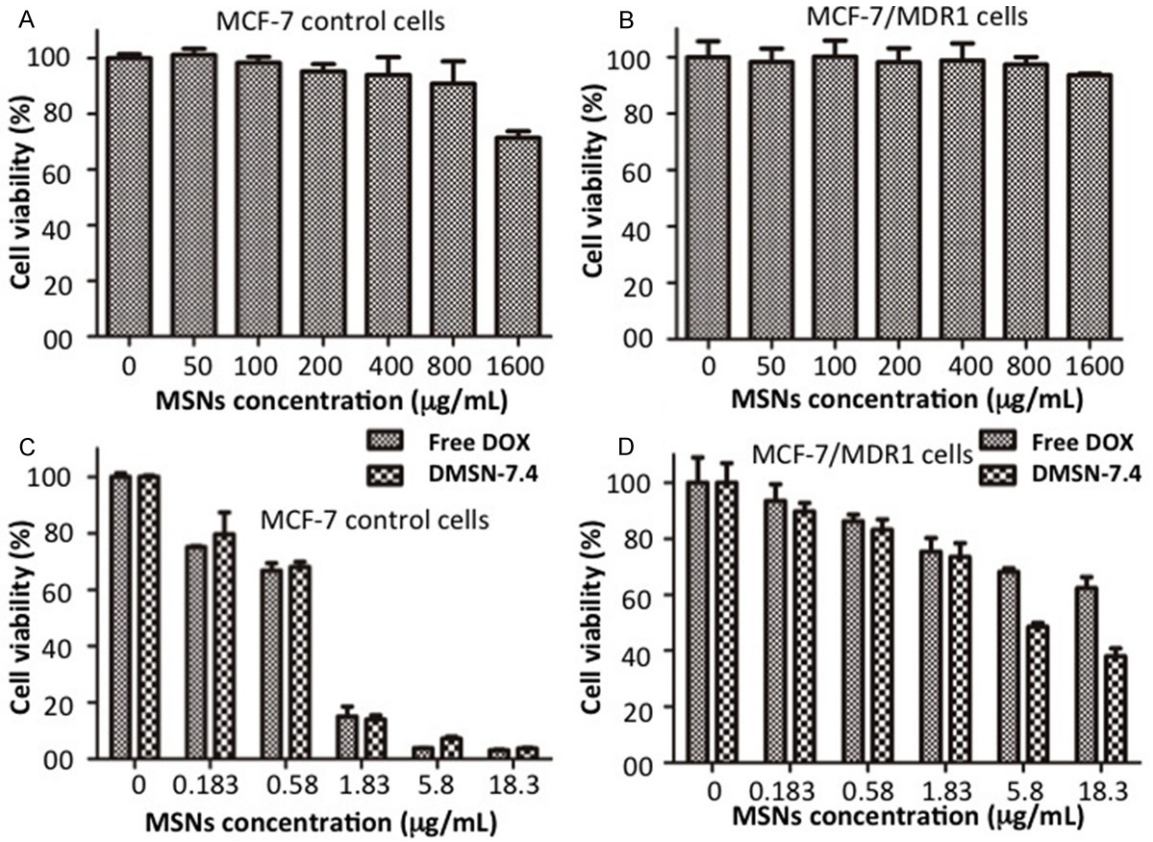

Figure 5. Cytotoxicity of the MSNs was measured by MTT in both MCF-7 and MCF-7/MDR1 cells at different concentrations. A. MSNs exhibited limited toxicity with 71.4% cell viability of MCF-7 cells at 1600 μg/mL and negligible cytotoxicity at 800 μg/mL or lower. B. MSNs exhibited no obvious cytotoxicity in MCF-7/MDR1 cells at the concentrations of 50 to 1600 μg/mL even after culturing for 48 h. C. No significant difference in cell viability of MCF-7 control cells after exposure to different concentrations of free DOX and DMSN-7.4. D. There is a significant difference in the viability of MCF-7/MDR1 cells at the concentrations of 5.8 and 18.3 (mg/mL) (P<0.001).

to MCF-7/MDR1 tumor-bearing mice. Five days after administration, the intratumoral DOX distribution was analyzed by DOX autofluorescence. As shown in **Figure 6A**, the free DOX group showed a small DOX signal similar to the saline group in the tumors, and the DMSN-7.4 group accumulated more DOX in the tumors, indicating retention of DMSN-7.4 in the tumor. At the end of the experiment, the free DOX group showed no significant tumor shrinkage, however, one mouse had pinhole-like skin damage induced by chemotherapy. The DMSN-7.4 group had a significantly reduced (34%) effect on the tumor weight of MCF-7/MDR xenografts in comparison with the saline group (**Figure 6B**).

Discussion

For the majority of patients with breast cancer, precision therapy with the combination of conventional cytotoxic anticancer drugs, endocrine therapeutic agents (tamoxifen), and immunological-based target therapy (monoclonal antibody trastuzumab) is necessary after radical mastectomy. Multidrug resistance to cytotoxic chemotherapy is the main cause of therapeutic failure and death in women with breast cancer. Although, several mechanisms have been identified to contribute to clinical drug-resistance in breast cancer, the problem of resistance to anticancer drugs has not disappeared. A novel approach to address cancer drug resistance is to use the advantages of nanocarriers to sidestep drug resistance mechanisms by endosomal delivery of chemotherapeutic agents [18, 19, 25].

In the present study, we demonstrated the use of a mesoporous silica nanoparticle drug loading system to overcome DOX resistance in

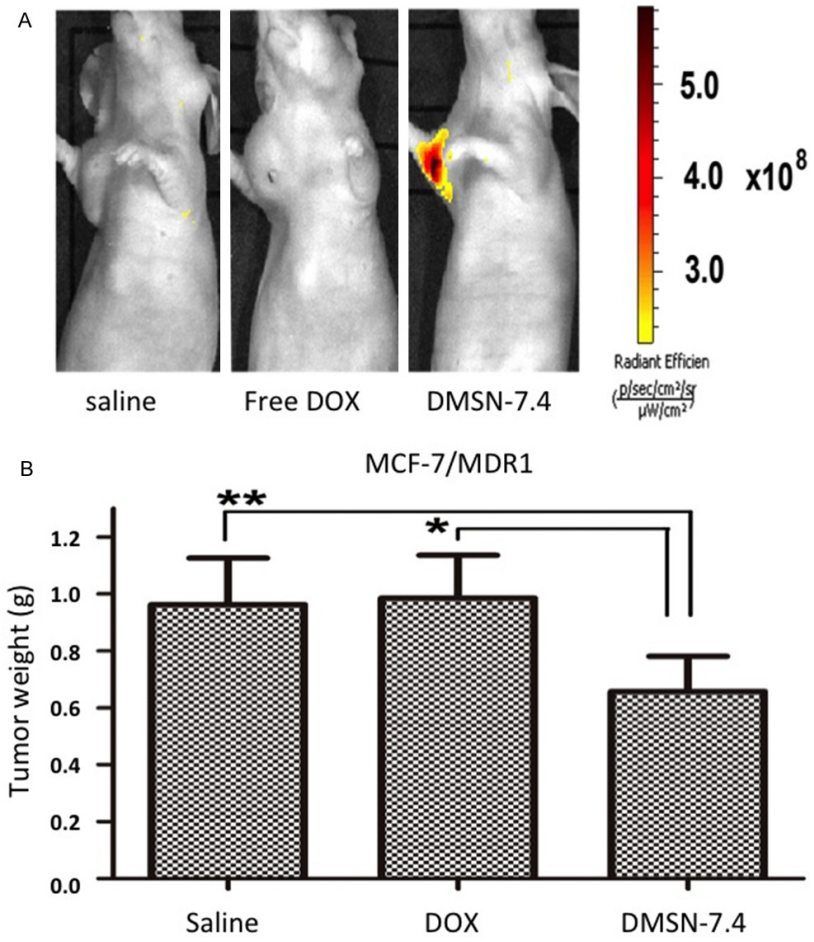

Figure 6. The MSNs-DOX drug delivery system increases therapeutic efficacy *in vivo.* A. The free DOX group showed as small DOX signal similar to the saline group in the tumors, and the DMSN-7.4 group accumulated more DOX in the tumors. B. The free DOX group showed no significant tumor shrinkage. The DMSN-7.4 group had a significant therapeutic effect as indicated by the tumor weights (*P<0.05, **P<0.01).

MDR1 human breast cancer MCF-7 cells and a MDR1 xenograft from the same cell line in nude mice by codelivering DOX. MCF-7 is a DOX sensitive breast cancer cell line. We successfully induced overexpression of MDR1 in MCF-7 cells by exposing cells to a gradient concentration of DOX. Drug resistance in MCF-7/MDR1 cells was confirmed by the detection of MDR1 mRNA and MDR1 protein using RT-PCR, western blot, immunohistochemical staining, and fluorescent immunochemistry staining.

We synthesized rod-like MSNs with a mean particle diameter of approximately 110 nm, uniform pore size of 2.7 nm and an aspect ratio (AR) of 2.1-2.5. We selected this type of rod-like MSN as the carrier for DOX delivery based on results reported by H Meng and colleagues [22]. They demonstrated that human cervical cancer (HeLa) cells and human lung cancer (A549) cells endocytose rod-shaped MSNs through a macropinocytosis process and have maximal uptake of these particles. Their data showed that rod-shaped particles determined the rate and abundance of MSNs uptake by the macropinocytosis process in cancer cell lines. MSNs with an AR of 2.1-2.5 were taken up in larger quantities compared to shorter or longer rods by this process. The rod-shaped MSNs synthesized in the present study had good efficacy for DOX delivery and good uptake by breast cancer MCF-7/MDR1 cells.

The natural fluorescence of DOX allows it to be tracked visually, and we observed the internalization of DOX-loaded rod-like nanoparticles (DMSN-7.4) and free DOX in vitro with fluorescence microscopy. DMSN-7.4 showed a higher intracellular DOX concentration than free DOX in MCF-7/MDR1 cells. This demonstrated that DMSN-7.4 can increase the intracellular DOX concentration with the assistance of active energy-dependent endocytosis of nanoparticles.

We found that DOX was highly uploaded into MSNs at physical pH (7.4) and released from nanoparticles at acidic pH. The tumor microenvironment is acidic (pH 5.8-7.6) and endosomes/lysosomes are acidic (pH 4-6). DOX was released more readily at pH less than 6.5. DOX release at acidic pH indicates that DOX is released preferentially in the endosomal/lysosomal compartment of cells where it is protected from drug efflux.

Conclusions

The use of nanotechnology for chemotherapeutic drug delivery in breast cancer treatment is a promising strategy to overcome drug resistance. Here, we demonstrate that drug resistance in a MDR1-overexpressed human breast cancer cell line can be overcome by treatment with DOX encapsulated within mesoporous silica nanoparticles.

Acknowledgements

We gratefully acknowledge financial support from the National Science Foundation of China (81371611, 81120108013, 81171391), National 973 Program (2014CB744504), and Jiangsu postdoctoral Fund Project (1102151C).

Disclosure of conflict of interest

None.

Address correspondence to: Jiandong Wang, Department of Pathology, Jinling Hospital, Nanjing University School of Medicine, Nanjing, 210002, China. E-mail: wangjd@aliyun.com; Guangming Lu, Department of Radiology, Jinling Hospital, Nanjing University School of Medicine, Nanjing 210002, China. E-mail: cjr.luguangming@vip.163.com

References

[1] Ferlay J, Shin HR, Bray F, Forman D, Mathers C and Parkin DM. Estimates of worldwide burden of cancer in 2008: GLOBOCAN 2008. Int J Cancer 2010; 127: 2893-2917.

[2] Yang X, Uziely B, Groshen S, Lukas J, Israel V, Russell C, Dunnington G, Formenti S, Muggia F and Press MF. MDR1 gene expression in primary and advanced breast cancer. Lab Invest 1999; 79: 271-280.

[3] Zyad A, Benard J, Tursz T, Clarke R and Chouaib S. Resistance to TNF-alpha and adriamycin in the human breast cancer MCF-7 cell line: relationship to MDR1, MnSOD, and TNF gene expression. Cancer Res 1994; 54: 825-831.

[4] Liu F, Liu S, He S, Xie Z, Zu X and Jiang Y. Survivin transcription is associated with P-glycoprotein/MDR1 overexpression in the multidrug resistance of MCF-7 breast cancer cells. Oncol Rep 2010; 23: 1469-1475.

[5] Xu D, Lu Q and Hu X. Down-regulation of P-glycoprotein expression in MDR breast cancer cell MCF-7/ADR by honokiol. Cancer Lett 2006; 243: 274-280.

[6] Mutoh K, Tsukahara S, Mitsuhashi J, Katayama K and Sugimoto Y. Estrogen-mediated post transcriptional down-regulation of P-glycoprotein in MDR1-transduced human breast cancer cells. Cancer Sci 2006; 97: 1198-1204.

[7] Tsubaki M, Komai M, Itoh T, Imano M, Sakamoto K, Shimaoka H, Takeda T, Ogawa N, Mashimo K, Fujiwara D, Mukai J, Sakaguchi K, Satou T and Nishida S. By inhibiting Src, verapamil and dasatinib overcome multidrug resistance via increased expression of Bim and decreased expressions of MDR1 and survivin in human multidrug-resistant myeloma cells. Leuk Res 2014; 38: 121-130.

[8] Kakumoto M, Sakaeda T, Takara K, Nakamura T, Kita T, Yagami T, Kobayashi H, Okamura N and Okumura K. Effects of carvedilol on MDR1-mediated multidrug resistance: comparison with verapamil. Cancer Sci 2003; 94: 81-86.

[9] Gong Y, Han W, Liu J, Chen F, Han J, Jin Y and Yong RO. Synergistic effects of verapamil and anti-mdr1 ribozyme on reversion of multidrug resistance in the P-glycoprotein-positive K562 cell line. Leukemia 2001; 15: 696-697.

[10] Abe T, Koike K, Ohga T, Kubo T, Wada M, Kohno K, Mori T, Hidaka K and Kuwano M. Chemosensitisation of spontaneous multidrug resistance by a 1,4-dihydropyridine analogue and verapamil in human glioma cell lines overexpressing MRP or MDR1. Br J Cancer 1995; 72: 418-423.

[11] Knezevic NZ and Lin VS. A magnetic mesoporous silica nanoparticle-based drug delivery system for photosensitive cooperative treatment of cancer with a mesopore-capping agent and mesopore-loaded drug. Nanoscale 2013; 5: 1544-1551.

[12] Shapira A, Davidson I, Avni N, Assaraf YG and Livney YD. beta-Casein nanoparticle-based oral drug delivery system for potential treatment of gastric carcinoma: stability, target-activated release and cytotoxicity. Eur J Pharm Biopharm 2012; 80: 298-305.

[13] Mortera R, Vivero-Escoto J, Slowing II, Garrone E, Onida B and Lin VS. Cell-induced intracellular controlled release of membrane impermeable cysteine from a mesoporous silica nanoparticle-based drug delivery system. Chem Commun (Camb) 2009; 3219-3221.

[14] Zhao Y, Trewyn BG, Slowing II and Lin VS. Mesoporous silica nanoparticle-based double drug delivery system for glucose-responsive controlled release of insulin and cyclic AMP. J Am Chem Soc 2009; 131: 8398-8400.

[15] Cho Y, Shi R, Borgens RB and Ivanisevic A. Functionalized mesoporous silica nanoparticle-based drug delivery system to rescue acrolein-mediated cell death. Nanomedicine (Lond) 2008; 3: 507-519.

[16] Pandey R and Khuller GK. Nanoparticle-based oral drug delivery system for an injectable anti-

biotic - streptomycin. Evaluation in a murine tuberculosis model. Chemotherapy 2007; 53: 437-441.

[17] Pandey R, Sharma A, Zahoor A, Sharma S, Khuller GK and Prasad B. Poly (DL-lactide-co-glycolide) nanoparticle-based inhalable sustained drug delivery system for experimental tuberculosis. J Antimicrob Chemother 2003; 52: 981-986.

[18] Zeng X, Morgenstern R and Nystrom AM. Nanoparticle-directed sub-cellular localization of doxorubicin and the sensitization breast cancer cells by circumventing GST-Mediated drug resistance. Biomaterials 2014; 35: 1227-1239.

[19] Meng H, Mai WX, Zhang H, Xue M, Xia T, Lin S, Wang X, Zhao Y, Ji Z, Zink JI and Nel AE. Codelivery of an optimal drug/siRNA combination using mesoporous silica nanoparticles to overcome drug resistance in breast cancer in vitro and in vivo. ACS Nano 2013; 7: 994-1005.

[20] Kievit FM, Wang FY, Fang C, Mok H, Wang K, Silber JR, Ellenbogen RG and Zhang M. Doxorubicin loaded iron oxide nanoparticles overcome multidrug resistance in cancer in vitro. J Control Release 2011; 152: 76-83.

[21] Yang S, Zhao L, Yu C, Zhou X, Tang J, Yuan P, Chen D and Zhao D. On the origin of helical mesostructures. J Am Chem Soc 2006; 128: 10460-10466.

[22] Meng H, Yang S, Li Z, Xia T, Chen J, Ji Z, Zhang H, Wang X, Lin S, Huang C, Zhou ZH, Zink JI and Nel AE. Aspect ratio determines the quantity of mesoporous silica nanoparticle uptake by a small GTPase-dependent macropinocytosis mechanism. ACS Nano 2011; 5: 4434-4447.

[23] Li Z, Likoko JN, Hwang AA, Ferris DP, Yang S, Derrien G, Charnay C, Durand JO and Zink JI. Measurement of Uptake and Release Capacities of Mesoporous Silica Nanoparticles Enabled by Nanovalve Gates. J Phys Chem C Nanomater Interfaces 2011; 115: 19496-19506.

[24] Jia Y, Tian W, Sun S, Han P, Xue W, Li M, Liu Y, Jiang S and Cui B. The influence of genetic polymorphisms in MDR1 gene on breast cancer risk factors in Chinese. Med Oncol 2013; 30: 601.

[25] Wen H, Guo J, Chang B and Yang W. pH-responsive composite microspheres based on magnetic mesoporous silica nanoparticle for drug delivery. Eur J Pharm Biopharm 2013; 84: 91-98.